



# Copper-iron mixed oxide supported onto cordierite honeycomb as a heterogeneous catalyst in the Kharasch-Sosnovsky oxidation of cyclohexene

M. Pilar Yeste<sup>a</sup>, M. Amine Fellak<sup>b</sup>, Hilario Vidal<sup>a,\*</sup>, Francisco M. Guerra<sup>c</sup>,  
F. Javier Moreno-Dorado<sup>c</sup>, José M. Gatica<sup>a</sup>

<sup>a</sup> Departamento de Ciencia de los Materiales e Ingeniería Metalúrgica y Química Inorgánica, Universidad de Cádiz, Puerto Real 11510, Spain

<sup>b</sup> Département de Génie des Matériaux, Université des Sciences et de la Technologie Mohamed Boudiaf, Oran, Algeria

<sup>c</sup> Departamento de Química Orgánica, Universidad de Cádiz, Puerto Real 11510, Spain

## ARTICLE INFO

### Keywords:

Allylic oxidation  
Copper-iron mixed oxide  
Cyclohexene  
Honeycomb monoliths  
Kharasch-Sosnovsky reaction

## ABSTRACT

A copper-iron mixed oxide was deposited by the washcoating procedure over cordierite honeycomb monoliths for its use as a heterogeneous catalyst in organic synthesis processes. In particular, the prepared catalyst, characterized by techniques such as X-ray fluorescence, X-ray diffraction, SEM-EDS, laser granulometry, adherence tests, Temperature-Programmed Oxidation and Temperature-Programmed Reduction, showed an excellent yield and stability in the selective production of the allylic ester derived from the Kharasch-Sosnovsky oxidation of cyclohexene with benzoic acid. The use of a structured catalyst here proposed opens up an interesting alternative to homogeneous catalysis in the field of synthetic chemistry.

## 1. Introduction

The Kharasch-Sosnovsky reaction has attracted the attention of synthetic chemists over the past few years since it enables the activation of C(sp<sup>3</sup>)-H allylic bonds through the catalytic action of different copper species [1–4]. This reaction was first published in 1958 by the authors after whom it is named [5–7]. They reported that some species of copper or cobalt catalyzed the oxidation of cyclohexene with *t*-butyl peroxybenzoate (PhCO<sub>3</sub>*t*-Bu). After its discovery, the reaction went somewhat unnoticed for some time. However, the current interest in C-H bond activation has brought this interesting reaction back to the fore. This interest has resulted in the development of asymmetric versions of the reaction by the groups of Denney [8], Muzart [9], and Feringa [10,11]. There is a short review by Brunel et al. [12] and another one by Eames and Watkinson [13], covering the most important features of the reaction, and a comprehensive review by Andrus and Lashley [14]. Recently our group published a review covering the main aspects reported up to 2016 [15]. Extensive mechanistic studies have also been performed by several authors [16–20].

However, two fundamental issues prevent the full incorporation of this reaction into the synthetic chemist's toolbox. On the one hand, it needs long reaction times, often days. On the other hand, it requires a large excess of the olefin to be oxidized and in fact, the yields are

expressed as a function of the oxidant. This fact is not acceptable when the olefin is a valuable substrate or is difficult to prepare.

In the heterogeneous mode, beyond some specific examples, the bibliography is scarce and the main challenge is selectivity [21–23]. The allylic oxidation of the olefin competes with the epoxidation of the double bond and the formation of over-oxidation products is a recurrent problem.

In a recent work, we have shown how honeycomb monoliths, integrally prepared from a mineral carbon, can act as a support of copper catalysts, leading to high yields (60–100% depending on the carboxylic acid used) in the preparation of allylic esters by Kharasch-Sosnovsky oxidation of cyclohexene [24]. Although some of the monoliths displayed fragile structural integrity, the study demonstrated the potential of this design. Unlike the homogeneous process, the use of a solid catalyst allowed avoiding complex procedures, simplifying the isolation of the products and the recycling of the catalyst. Moreover, being unitary structures, the monoliths offered the additional advantage of simpler handling, while their honeycomb design maximized the contact between the flow of reactant molecules and the active sites of the catalyst.

On the other hand, in a previous study, we used a mixed oxide of copper and iron as an efficient heterogeneous catalyst in other organic synthesis reactions such as the acyloxylation of 1,4-dioxanes and 1,4-

\* Corresponding author.

E-mail address: [hilario.vidal@uca.es](mailto:hilario.vidal@uca.es) (H. Vidal).

<https://doi.org/10.1016/j.cattod.2021.10.020>

Received 2 February 2021; Received in revised form 21 July 2021; Accepted 20 October 2021

Available online 27 October 2021

0920-5861/© 2021 The Author(s). Published by Elsevier B.V. This is an open access article under the CC BY-NC-ND license (<http://creativecommons.org/licenses/by-nc-nd/4.0/>).

dithianes [25], after having found that doping copper with aluminum can provide the synergistic action of two different metallic centers [26].

With the above precedents, in this study, we have prepared a mixed oxide of copper and iron to be deposited on cordierite honeycomb monoliths with a mechanical resistance superior to the previously described for those made of carbon, in order to test them in the same reaction in which only pure copper oxides were employed. Benzoic acid **2** was chosen as model carboxylic acid for the Kharasch-Sosnovsky oxidation of cyclohexene **1** according to Fig. 1.

## 2. Experimental

### 2.1. Catalysts preparation

The copper-iron mixed oxide (CuFeOx) was prepared following the procedure previously employed for the synthesis of a copper-aluminum mixed oxide [26], also reported in [27]. The selected Cu/Fe nominal molar ratio was 1:1, after having found in the previous study in which different compositions were prepared for the catalytic use in the CO-PROX reaction that this was among the most active ones and that a mixed phase was formed [27]. Briefly, an aqueous solution of Na<sub>2</sub>CO<sub>3</sub> (1.27 g) and NaOH (5.20 g) was dropped onto another one containing CuCl<sub>2</sub> (2.02 g, 0.015 mol) and FeCl<sub>3</sub>·6H<sub>2</sub>O (4.05 g, 0.015 mol) in 50 mL of water. The resulting dark brown suspension was stirred at 70 °C for 22 h, filtered, and washed with boiling water (3×200 mL), being further dried in an oven at 105 °C for 24 h. Three batches were prepared following the same recipe and the use of X-ray fluorescence (XRF) allowed us to check the reproducibility in the composition of the samples obtained (Table 1).

Considering the similar composition of the lots obtained, they were mixed and milled using a CryoMill from Retsch (20 Hz, 4 h) in order to decrease the average size of grain from 22 down to 4 μm (Fig. 2) to further facilitate the adherence of this powder onto a monolithic substrate [28].

The main properties of a CuFeOx powdered sample prepared similarly were reported in a previous study [27]. The characterization evidenced its mesoporous character and the similar composition estimated by different techniques, which matched quite well the nominal Cu/Fe molar ratio. In addition, the structural analysis by both X-ray diffraction (XRD) and Raman spectroscopy confirmed the coexistence of a spinel stoichiometric mixed phase (CuFe<sub>2</sub>O<sub>4</sub>) along with fractions of pure copper and iron oxides.

In this work, the structured catalyst (CuFeOx monolith) was prepared following the washcoating procedure, widely described in the literature [29]. We started from blocks of 230 cps commercial cordierite from Corning that were cut to obtain cylinder pieces having 13 mm of diameter, 47 mm of length, and approx. 2 g of weight. These honeycomb monoliths were immersed at 3 cm/min, during 90 s (the first 15 s under ultrasounds), in a stabilized at pH 4 and continuously stirred slurry containing the copper-iron mixed oxide powder (19.1 wt%), PVA (1.7 wt%), and Nyacol AL20 colloidal alumina (4.2 wt%). This slurry had a viscosity of 26 CP, a value that is within the optimum range (5–30 CP) for this kind of preparation [28]. The pH was selected in accordance with the Z potential curve (Fig. 3), for which pH was fitted with acetic acid or ammonia. According to the literature [28], Z potential absolute values higher than 20 mV lead to stable suspensions.

After the controlled immersion, the monoliths were dried first by air

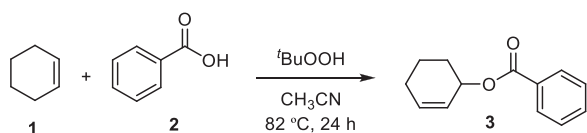


Fig. 1. Kharasch-Sosnovsky oxidation of cyclohexene **1** used as benchmark reaction.

Table 1

Elemental analysis (wt%) of different batches of the prepared copper-iron mixed oxide powder as obtained by XRF.

Sample	Cu	Fe	O
CuFeOx (2.6 g)	42.8	39.7	17.5
CuFeOx (9.2 g)	40.7	41.0	18.3
CuFeOx (9.9 g)	42.1	40.2	17.7

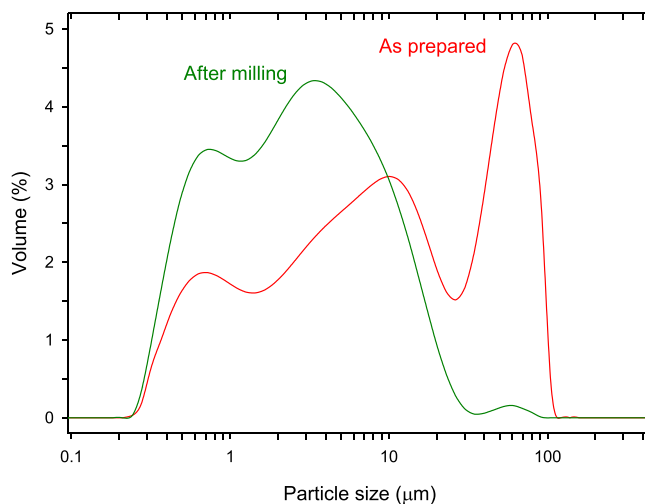


Fig. 2. Granulometric analysis using a Mastersizer 2000 granulometer (Malvern), operating with laser diffraction and previous ultrasonication of the samples in deionised water during 5 min, of the copper-iron mixed oxide (CuFeOx) powder as prepared and after milling.

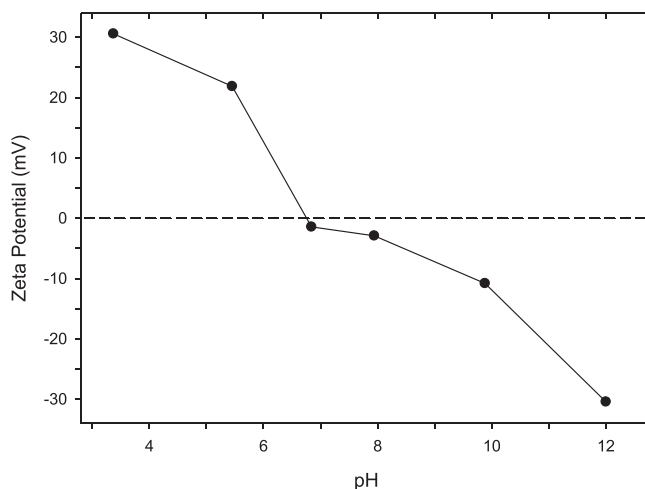
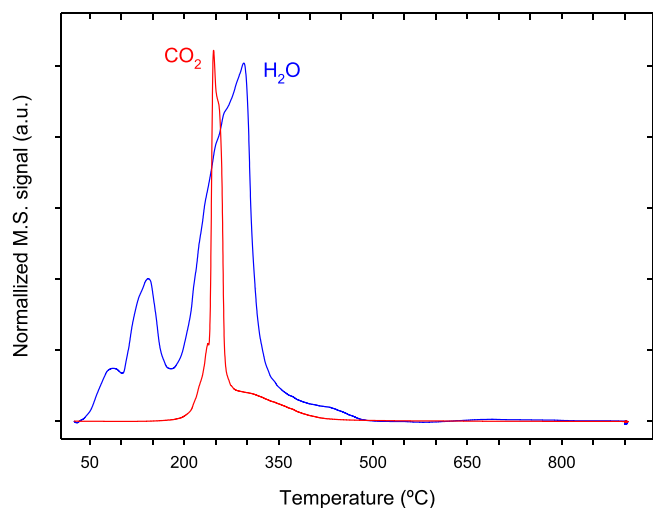


Fig. 3. Z potential vs pH for the slurry containing the CuFeOx powder.

blowing off the slurry excess and then in an oven at 120 °C for 30 min. The final weight gain was approx. 100 mg/g. Finally, the monoliths were calcined at 550 °C for 1 h, treatment that was also applied to the powder resulting from the remaining slurry, which was led to dryness to produce the reference CuFeOx-S sample. This treatment was selected based on a previous Temperature-Programmed Oxidation (TPO) experiment (Fig. 4) to ensure complete decomposition of the catalyst precursors and to enhance the washcoat adherence to the monolith [30]. In fact, this resulted to be higher than 94% as estimated from the standard procedure consisting of measuring the weight loss after applying ultrasounds for 30 min in petroleum ether [29].



**Fig. 4.** TPO signals recorded by Mass Spectrometry (Pfeiffer QMS-200-D-35614) for the CuFeOx-S sample under O<sub>2</sub>(5%)/He at a heating rate of 10 °C/min.

## 2.2. Catalysts characterization

The copper and iron content was determined by XRF using a Bruker S4 Pioneer diffractometer, equipped with area detection (CCD) and Kyoflex cryostatic systems.

XRD analyses were performed at room temperature on a Bruker D8 Advance powder diffractometer operating with Cu K<sub>α</sub> radiation (scanning steps of 0.05°, counting time of 20 s). In the particular case of the honeycomb monolithic samples Grazing Incidence X-Ray Diffraction (GIXRD) analysis was applied as a way to maximize the active phase peaks in coated materials. In order to analyze the phase composition of the samples, average crystal size, and lattice parameters the Powder Cell software was used.

Scanning Electron Microscopy (SEM) images and Energy Dispersive Spectroscopy (EDS) data were obtained using a FEG Nova NanoSEM 450 microscope operating at 30 kV.

Finally, H<sub>2</sub> Temperature-Programmed Reduction (H<sub>2</sub>-TPR) profiles were recorded in an Autochem II 2920 equipped with thermal conductivity detector (TCD), operating with a 25 mL/min flow of H<sub>2</sub>(5%)/Ar and at 10 °C/min as heating rate. A maximum temperature of 900 °C was reached, which was further maintained for 1 h as an isothermal step until recovering the baseline in the corresponding H<sub>2</sub> consumption signals. Before the experiments, the samples were pre-treated under He (25 mL/min) at 150 °C for 1 h.

## 2.3. Activity testing

All reagents were purchased from Aldrich or PANREAC and were used without further purification.

### 2.3.1. General procedure for the Kharasch-Sosnovsky allylic oxidation of cyclohexene

An initial experiment employing only the powdered catalyst was performed. The powder (8–21 mg) was suspended in acetonitrile (3 mL) in a 25 mL heavy-walled cylindrical reaction flask. Benzoic acid (1.0 mmol) was then added and the mixture was vigorously stirred for 10 min. Cyclohexene (4 mmol) and *t*-BuOOH (1.5 mmol, 70% solution in water) were added. The mixture was stirred at 82 °C for 24 h, after which time, a saturated aqueous solution of Na<sub>2</sub>SO<sub>3</sub> (10 mL) was added. The solution was extracted with EtOAc (3×10 mL), washed with a saturated aqueous brine solution (10 mL), and dried over anhydrous Na<sub>2</sub>SO<sub>4</sub>. The solvent was removed by rotary evaporation and the resulting residue was purified by silica gel column chromatography

employing a 1:19 mixture of EtOAc:petroleum ether as eluent.

### 2.3.2. General procedure for the Kharasch-Sosnovsky allylic oxidation of cyclohexene employing the honeycomb monoliths

The reaction was carried out in a Thiele tube immersed in a heating bath in an assembly similar to that described in reference [24]. The shape of the Thiele tube ensured the recirculation of the solvent along the monolith, which was inserted into the wider arm of the tube. A Liebig condenser completed the setup. CH<sub>3</sub>CN (30 mL) was poured into the tube to hold the reaction mixture. Then, benzoic acid (10 mmol), cyclohexene (40 mmol), and *t*-BuOOH (15 mmol, 70% solution in water) were added. The reaction was worked up and the product purified as described above. The monolith was recovered, thoroughly washed with acetonitrile, and left to dry prior to the following cycle. Similar reactions were carried out with *p*-methylbenzoic acid, *p*-methoxybenzoic acid, *p*-chlorobenzoic acid, and *p*-nitrobenzoic acid.

In the case of benzoic acid, an additional system was assembled, consisting of a peristaltic pump that drove the solvent with a flow rate of 30 mL/min in a closed circuit. CH<sub>3</sub>CN (120 mL) was poured into a tank to hold the reaction mixture. Benzoic acid (10 mmol, 1.22 g), cyclohexene (40 mmol, 4.08 mL), and *t*-BuOOH (15 mmol, 1.93 mL of a 70% solution in water) were added. The monolith was placed in a separate but connected thermostatic reactor. Fig. 5 illustrates the whole set up in the case of the experiments carried out with an entire monolith. The reaction was run again at 82 °C, and after 24 h it was worked up and the product purified as described above.

The products were identified by Nuclear Magnetic Resonance (NMR) using an Agilent 400 MR instrument. Mass spectra were recorded employing a Bruker Scion GC-TQ gas chromatograph coupled to a Bruker TQ mass spectrometer. GC analyses were performed in a Perkin-Elmer Clarus 400 chromatograph using a DB-5 column.

## 3. Results and discussion

### 3.1. Compositional characterization by X-Ray microfluorescence

Results obtained by XRF analysis of the structured catalyst are shown in Fig. 6. As can be seen, the study of up to 100 different areas of the monolith walls demonstrates that the surface composition of the wash-coat is quite homogeneous in terms of both copper and iron contents. Moreover, their average mean ratio is close to the nominal value of 1 when they are expressed in moles. Both observations are aligned with the target of the preparation procedure.

### 3.2. SEM-EDS study

The SEM technique allowed obtaining images of different areas of the monolith walls, which illustrate the uniform coating of the support

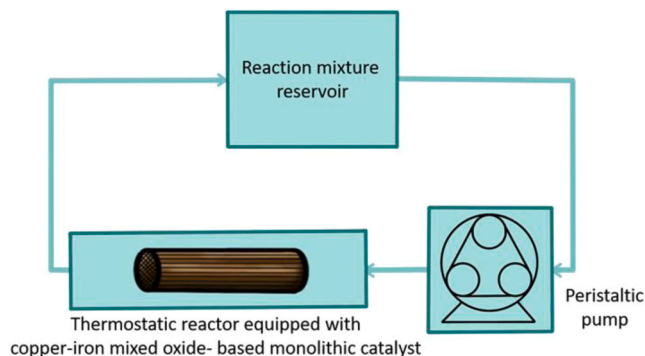


**Fig. 5.** Scheme of the experimental set up in the catalytic tests performed using copper-iron mixed oxide-based monolithic catalysts in the Kharasch-Sosnovsky oxidation of cyclohexene.

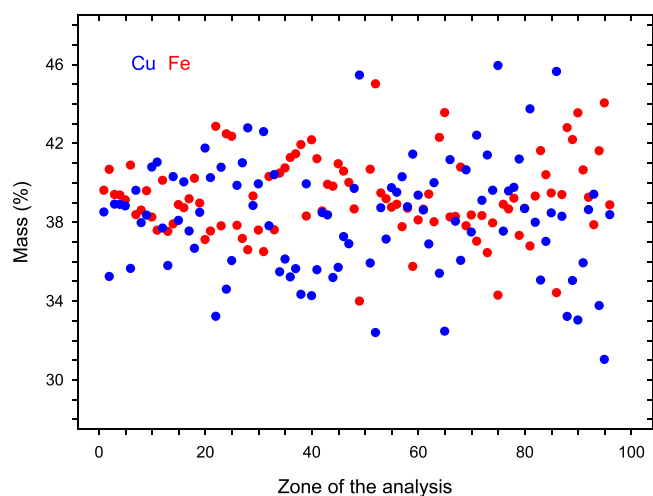


**Fig. 6.** Elemental composition obtained by XRF analysis over 1.47 mm×1.10 mm rectangle zones of the CuFeOx monolith. The mean average composition for this study resulted to be 39.2 and 38.4 wt% for Fe and Cu, respectively.

by the deposited copper-iron oxide. Complementary EDS spectra showed clearly the peaks attributable to iron and copper along with those corresponding to the characteristic elements of cordierite. Furthermore, this surface analysis also provided values for the Cu/Fe ratio in relatively good agreement with the nominal composition and the analysis performed by XRF. In addition, surface elemental distribution obtained by EDS mapping for copper and iron demonstrated that the spatial location of the two metals is practically the same in the analyzed areas, which suggests at least good physical contact between them. All these results can be observed in Fig. 7.

### 3.3. Structural characterization by XRD

Fig. 8 shows the diffractograms obtained for the studied catalyst both in the form of powder and supported onto a cordierite monolith. The diagram corresponding to the powder derived from the slurry is also included as a reference. In all cases, the samples were calcined at 550 °C 1 h. As can be noticed, almost no differences are observed between the starting powder and that obtained from the dried remaining slurry, which contains colloidal alumina. In both cases peaks characteristic of the tenorite phase of copper oxide are detected, the most intense ones, as

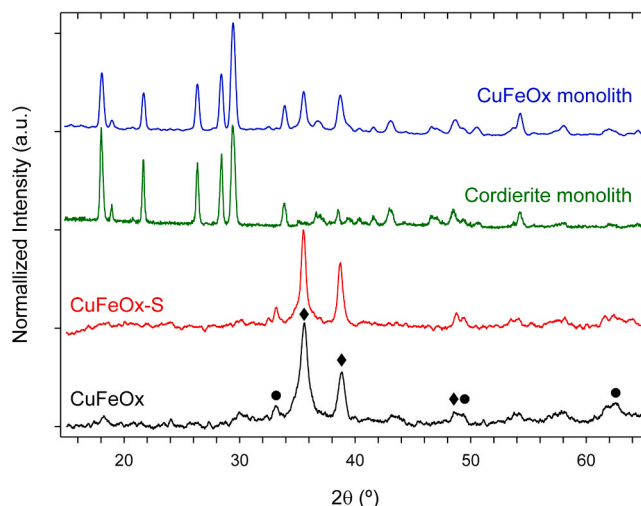


**Fig. 8.** X-ray diffractograms of the studied samples. The diagrams have been shifted in the Y-scale for the sake of clarity and the position of the main peaks attributed to CuO tenorite (◆) and Fe<sub>2</sub>O<sub>3</sub> hematite (●) are marked.

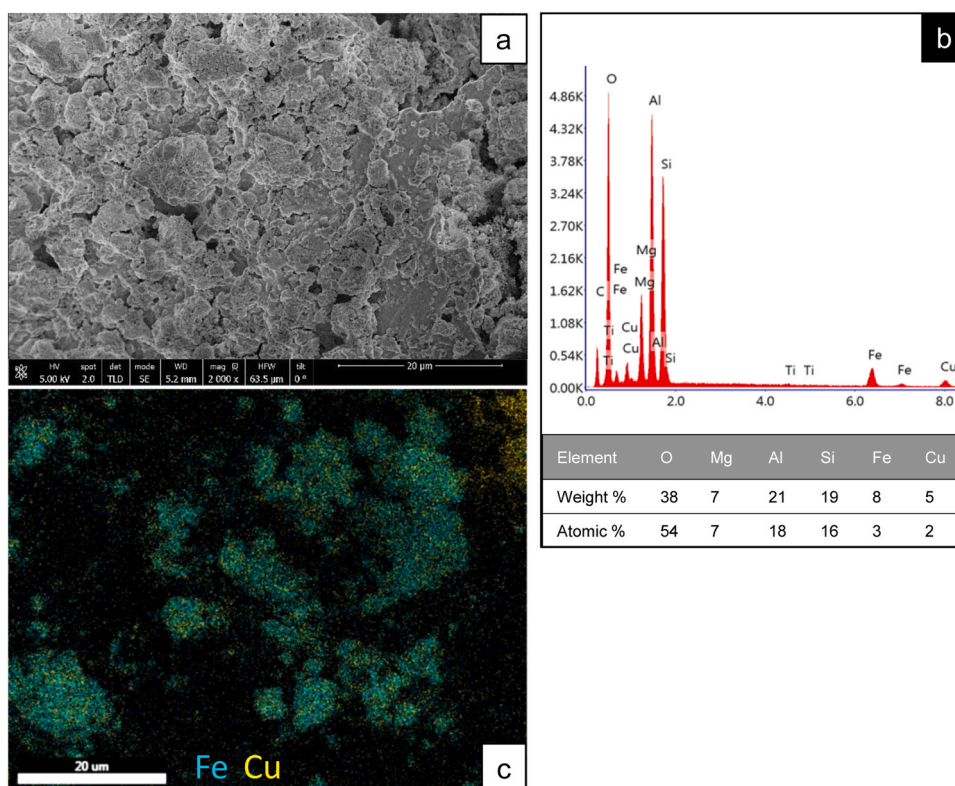


**Fig. 7.** SEM image (a) and the corresponding EDS spectrum in scan mode (b) of a wall piece of the copper-iron oxide washcoated monolith. The compositional mapping for Fe and Cu obtained through EDS analysis of other part of the same sample is presented in (c).

found in previous studies with copper-iron mixed oxides [27]. Regarding the peaks with lower intensity, especially those located at  $2\theta$  values between  $55^\circ$  and  $70^\circ$ , they can be attributed to the hematite phase of iron sesquioxide. On the other hand, in the monolithic catalysts, besides the above, those assignable to cordierite can be clearly observed. The peaks assignable to  $\text{CuFe}_2\text{O}_4$  can be only revealed when performing complementary fine Rietveld analysis as previously observed for the powdered catalyst [25].

Besides, average crystal sizes and lattice parameters for the three samples were estimated using the Powder Cell software as summarized in Table 2. No significant changes were found except slight variations in the lattice parameters corresponding to the alumina-containing samples.

### 3.4. TPR investigation

To get more insights on the possible interaction between copper and iron, TPR experiments were carried out considering their particular sensitiveness to the metal phase nature. The signals corresponding to the  $\text{H}_2$  consumption and consequent reduction of the copper and iron phases in the catalyst are presented in Fig. 9. Again, those obtained in the experiments performed with the starting  $\text{CuFeOx}$  powder,  $\text{CuFeOx-S}$  reference, and  $\text{CuFeOx}$  monolith are compared.

Notice first that the reduction profiles are similar to those previously observed for copper-iron mixed oxides [27]. Although the analysis of the TPR profiles is complex, the wide peak below  $500^\circ\text{C}$  in the powdered catalyst must correspond to the typical reduction of the  $\text{CuO}$  tenorite phase, in good agreement with the XRD analysis. In this sense, its shift to lower temperatures in the  $\text{CuFeOx-S}$  sample suggests that the presence of alumina in the slurry favors copper reducibility. A similar effect was previously observed in our lab studying cobalt catalysts doped with  $\text{La-CeO}_2$  [29]. On the contrary, the less intense and much extended signal at higher temperatures in both samples,  $\text{CuFeOx}$  and  $\text{CuFeOx-S}$ , should be related to the reduction of different iron oxide species.

In the case of the monolithic catalyst, it is remarkable that the two above signals seem to shift toward lower temperature, giving an intense peak slightly below  $300^\circ\text{C}$  and another one less intense but wider, centered around  $450^\circ\text{C}$ , which might correspond to the reduction of copper and iron cations, respectively. These results suggest that along with big crystals of copper oxide onto the monolith substrate, as indicated by the X-ray diffractogram, there must be a mixed oxide as part of the active phase of the catalyst, also available for the reaction.

### 3.5. Catalytic activity

The first step in the study of the catalytic performance was taken by analyzing the response of the samples in the form of powder. As can be observed in Table 3, the prepared copper-iron mixed oxide, even diluted with alumina in the same proportion employed for its further deposition onto the monoliths by washcoating (Section 2.1), resulted more active than any of the pure oxides, considered separately, prepared in the same manner as reference samples. Moreover, it showed also higher activity than a physical mixture of both. This confirmed the interaction between the two metals, pointed out by the previous characterization, and encouraged for the second step, the catalyst evaluation upon deposition

**Table 2**

Data obtained by analysis of the X-Ray diffractograms using the Powder Cell software.

Sample	Crystal size (nm)	Lattice parameter (Å)				
		CuO			$\text{Fe}_2\text{O}_3$	
		a	b	c	a=b	c
$\text{CuFeOx}$	28	4.654	3.409	5.112	5.023	13.709
$\text{CuFeOx-S}$	35	4.655	3.411	5.108	5.023	13.701
$\text{CuFeOx}$ monolith	30	4.648	3.411	5.108	5.024	13.703

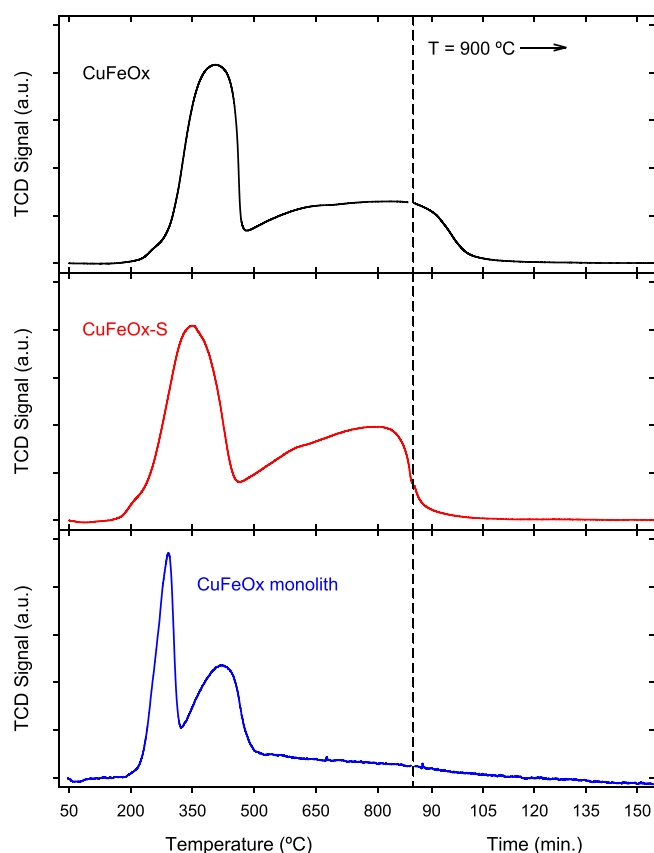


**Fig. 9.** TPR diagrams showing  $\text{H}_2$  consumption denotative of reduction in the studied samples (around 1 cm long cylinder in the case of the monolith). For the sake of comparison, the intensity of the curves has been normalized by the  $\text{CuFeOx}$  amount in each sample.

**Table 3**

Allylic oxidation of cyclohexene over the powdered catalysts.

Catalyst	Weight (mg) <sup>a</sup>	Amount of cyclo-hex-2-enil benzoate obtained (mg)	Yield (%) <sup>b</sup>
$\text{CuO}$	7.96	96	48
$\text{Fe}_2\text{O}_3$	7.99	0	0
$\text{CuO} + \text{Fe}_2\text{O}_3^c$	7.76+7.99	102	51
$\text{CuFeOx}$	21	141	70
$\text{CuFeOx} + \text{Al}_2\text{O}_3^c$	21.5+4.7	139	69

<sup>a</sup> The weight of the catalyst was selected to ensure comparable copper and/or iron moles amount. All tests were carried out using benzoic acid (1.0 mmol), cyclohexene (4.0 mmol), *t*-BuOOH (1.5 mmol), refluxing  $\text{CH}_3\text{CN}$  (3 mL), 24 h at  $82^\circ\text{C}$ .

<sup>b</sup> Isolated yields. <sup>c</sup>Physical mixture.

onto the cordierite monoliths. In this regard, as detailed in the experimental section, the setup was changed to a flow recirculation to take advantage of the honeycomb design. However, the rest of the parameters such as the molar proportion of the reagents was kept in order to allow the comparison between the tests performed with powders and those operating with monoliths.

Fig. 10 shows the result of submitting a  $\text{CuFeOx}$ -washcoated monolith to five consecutive cycles of reaction. Taking into account that the reagents mixture was renewed after each cycle, several remarks are noteworthy. First, notice how the yield was kept around an average value of 80%, which is even higher than that of the powdered  $\text{CuFeOx}$  with an equivalent amount of active phase (Table 3). Second, the monolith weight also remained almost constant during all the tested cycles. Moreover, no leaching effects, whose occurrence would have led

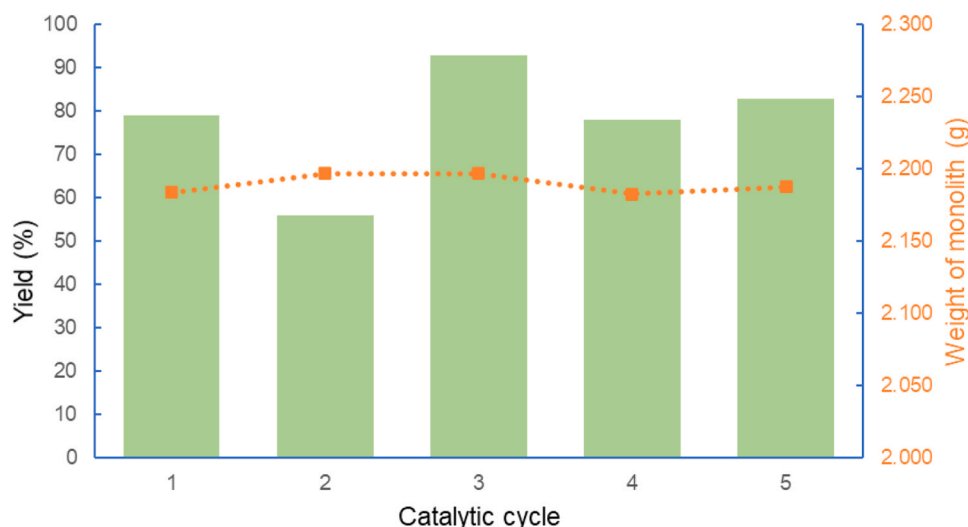


**Fig. 10.** Isolated yields obtained in consecutive cycles of the allylic oxidation of cyclohexene over a CuFeOx-washcoated monolithic catalyst, and variation of the monolith weight. Reactions were carried out in a Thiele tube as described in the experimental part. The reagents mixture was renewed after each cycle. All reaction cycles were carried out using benzoic acid (10 mmol), cyclohexene (40 mmol), *t*-BuOOH (15 mmol), CH<sub>3</sub>CN (30 mL), with reflux for 24 h at 82 °C.

to the typical blue colouration of the liquid medium due to the solvated Cu (II) ions, were observed. Finally, no structural damages were observed in the monoliths, unlike those previously reported where the support was carbon [24]. This fact confirmed the expected higher resistance and consequent advantage of cordierite. In summary, all these observations point to the superior stability of the monolithic catalyst prepared in this work.

At this point, we found interesting to verify the behavior of the monolith in the oxidation of cyclohexene in the presence of other related benzoic acid derivatives to determine the existence of any polar effect caused by different functional groups in the aromatic ring. To this end, the substrates listed in Table 4 were tested. The table reveals that the presence of donor groups such as a *p*-methyl or a *p*-methoxyl group (entries 1 and 2) favors the reaction, which takes place with excellent yields (5, *p*-Me, 85%; 7, *p*-OMe, 94%). The presence of a deactivating group on the ring such as in the cases of *p*-chlorobenzoic acid and *p*-nitrobenzoic acid (entries 3, and 4, respectively) causes a decrease in the yield of the reaction, leading to esters 9 and 11 in a 68% and 55% yield. Attempting to increase the yield by adding more oxidant led to the appearance of 3-(*tert*-butoxy)cyclohex-1-ene, resulting from the incorporation of a *t*-butoxy group from *t*-BuOOH. This evidence points to the fact that the electron density of the aromatic ring plays a decisive role in the outcome of the reaction.

Finally, we decided to carry out an optimized dynamic experiment to see whether it was possible to reproduce the result achieved on a larger scale. For this purpose, the system shown in Fig. 5 was assembled, where the catalyst monolith was introduced into a heated glass cylinder, which acts as a reactor, connected to a reservoir where the bulk of the reaction was found. The solvent was driven by a peristaltic pump with a flow of 30 mL/min that was forced through the channels of the monolith. The reaction was carried out using cyclohexene and benzoic acid under the same conditions described above. The reaction produced cyclohexenyl benzoate 3 (Fig. 1) in an 84% yield.

The approach of using monolithic devices offers certain advantages over the use of free powder catalyst. While in the latter case, clogging of the filters frequently occurs, in our case, the removal of the monolithic unit is trivial, which avoids tedious filtrations. On the other hand, in such an assembly, it is simpler to replace either the monolith when its catalytic capacity is depleted, or the rest of the reagents when the reaction is considered to have reached its completion. These two factors constitute a good starting point for the development of methods that work in continuum and for the implementation of reactions on a larger

**Table 4**

Influence of the presence of a functional group in the oxidation reaction.

Entry	Substrate	Product	Yield <sup>a</sup>
1			85 %
2			94 %
3			68 %
4			55 %

Reactions were carried out in a Thiele tube as described in the experimental part. Cyclohexene (1 mmol), carboxylic acid (4 mmol) in CH<sub>3</sub>CN (6 mL), reflux, 24 h. Isolated yield after one cycle.

FIGURE CAPTIONS

scale.

#### 4. Conclusions

A catalyst based on copper-iron mixed oxide with 1:1 molar ratio stoichiometry was prepared by the co-precipitation method from chloride precursors, ending with a calcination treatment at 550 °C for 1 h. The obtained powdered sample was deposited by washcoating over commercial cordierite honeycomb monoliths, leading to uniform and compositionally homogeneous coatings with appropriate adherence

(>94%). In addition, characterization by X-ray diffraction and Temperature-Programmed Reduction suggested that the catalyst active phase must consist of a fraction of mixed phase coexisting with parts in the form of pure oxides (CuO and Fe<sub>2</sub>O<sub>3</sub>). In any case, the monolithic catalyst exhibited a high yield (around 80%) in the Kharasch-Sosnovsky oxidation of cyclohexene employing benzoic acid. Furthermore, the structured catalyst showed high stability, not finding signs of copper lixiviation or mechanical defects after several consecutive cycles of reaction.

The above results appear as promising as they come from an experimental procedure that is innovative when compared to the conventional way of carrying out the process, via homogeneous catalysis. On one hand, the use of a flow recirculation over a structured catalyst allows an intensification of the process. On the other hand, it represents a more environmentally friendly route by simplifying steps and generating fewer residues. Finally, yet importantly, it inspires to test the honeycomb design with other organic synthesis processes, with a special interest for those implying C-H bond activation.

### CRedit authorship contribution statement

**M. Amine Fellak:** Investigation. **José M. Gatica:** Conceptualization, Methodology, Writing – review & editing, Supervision. **M. Pilar Yeste:** Investigation. **Francisco M. Guerra:** Conceptualization, Methodology, Funding acquisition. **F. Javier Moreno-Dorado:** Investigation, Resources. **Hilario Vidal:** Conceptualization, Methodology, Writing – original draft preparation, Supervision.

### Declaration of Competing Interest

The authors declare that they have no known competing financial interests or personal relationships that could have appeared to influence the work reported in this paper.

### Acknowledgments

The authors thank the Ministry of Economy and Competitiveness of Spain (Projects MAT2017-85-719-R, and AGL2017-88083-R), the Junta de Andalucía (FQM-110 and FQM-169 groups), and the Institute of Electron Microscopy and Materials (IMEYMAT) of Cadiz University (UCA) (Projects HOMOGREEN and NUPRECAT) for their financial support. They also acknowledge the SC-ICYT of the UCA for using its XRD NMR, and electron microscopy division facilities.

### References

- [1] A. Levina, J. Muzart, Enantioselective allylic oxidation in the presence of the Cu(I)/Cu(II)-Proline catalytic system, *Tetrahedron* 6 (1) (1995) 147–156, [https://doi.org/10.1016/0957-4166\(94\)00370-Q](https://doi.org/10.1016/0957-4166(94)00370-Q).
- [2] J. Eames, M. Watkinson, Catalytic allylic oxidation of alkenes using an asymmetric Kharasch–Sosnovsky reaction, *Angew. Chem. Int. Ed.* 40 (19) (2001) 3567–3571, [https://doi.org/10.1002/1521-3773\(20011001\)40:19%3C3567::aid-anie3567%3E3.0.co;2-c](https://doi.org/10.1002/1521-3773(20011001)40:19%3C3567::aid-anie3567%3E3.0.co;2-c).
- [3] M.B. Andrus, J.C. Lashley, Copper catalyzed allylic oxidation with peresters, *Tetrahedron* 58 (2002) 845–866, [https://doi.org/10.1016/S0040-4020\(01\)01172-3](https://doi.org/10.1016/S0040-4020(01)01172-3).
- [4] A.L. García-Cabeza, R. Marín-Barrios, F.J. Moreno-Dorado, M.J. Ortega, G., M. Massanet, F.M. Guerra, Allylic oxidation of alkenes catalyzed by a copper–aluminum mixed oxide, *Org. Lett.* 16 (2014) 1598–1601, <https://doi.org/10.1021/ol500198c>.
- [5] M.S. Kharasch, G. Sosnovsky, The reactions of *t*-butyl perbenzoate and olefins – a stereospecific reaction, *J. Am. Chem. Soc.* 80 (1958) 756, <https://doi.org/10.1021/ja01536a062>.
- [6] M.S. Kharasch, A. Fono, A modification of free radical reactions, *J. Org. Chem.* 23 (1958) 324–325, <https://doi.org/10.1021/jo01096a624>.
- [7] M.S. Kharasch, G. Sosnovsky, N.C. Yang, Reactions of *t*-Butyl peresters. I. The reaction of peresters with olefins, *J. Am. Chem. Soc.* 81 (1959) 5819–5824, <https://doi.org/10.1021/ja01530a067>.
- [8] D.B. Denney, R. Napier, A. Cammarata, A convenient method for the preparation of some optically active allylic alcohols, *J. Org. Chem.* 30 (1965) 3151–3153, <https://doi.org/10.1021/jo01020a066>.
- [9] J. Muzart, Oxidation of alkenes: metal induced formation of an allylic carbon-oxygen bond, *Bull. Soc. Chim. Fr.* (1986) 65–77.
- [10] M.T. Rispens, C. Zondervan, B.L. Feringa, Catalytic enantioselective allylic oxidation, *Tetrahedron Asymmetry* 6 (1995) 661–664, [https://doi.org/10.1016/0957-4166\(95\)00054-S](https://doi.org/10.1016/0957-4166(95)00054-S).
- [11] C. Zondervan, B.L. Feringa, Remarkable reversal of the non-linear effect in the catalytic enantioselective allylic oxidation of cyclohexene using copper proline complexes and *t*-butyl hydroperoxide, *Tetrahedron Asymmetry* 7 (1996) 1895–1898, [https://doi.org/10.1016/0957-4166\(96\)00224-8](https://doi.org/10.1016/0957-4166(96)00224-8).
- [12] J.M. Brunel, O. Legrand, G. Buono, Recent advances in asymmetric copper allylic oxidation of olefins, *C. R. Acad. Sci. Ser. Lic.* 2 (1) (1999) 19–23, [https://doi.org/10.1016/S1387-1609\(99\)80033-4](https://doi.org/10.1016/S1387-1609(99)80033-4).
- [13] J. Eames, M. Watkinson, Catalytic allylic oxidation of alkenes using an asymmetric Kharasch–Sosnovsky reaction, *Angew. Chem. Int. Ed.* 40 (2001) 3567–3571, [https://doi.org/10.1002/1521-3773\(20011001\)40](https://doi.org/10.1002/1521-3773(20011001)40).
- [14] M.B. Andrus, J.C. Lashley, Copper catalyzed allylic oxidation with peresters, *Tetrahedron* 58 (2002) 845–866, [https://doi.org/10.1016/S0040-4020\(01\)01172-3](https://doi.org/10.1016/S0040-4020(01)01172-3).
- [15] A.L. García-Cabeza, F.J. Moreno-Dorado, M.J. Ortega, F.M. Guerra, Copper-catalyzed oxidation of alkenes and heterocycles, *Synthesis* 48 (2016) 2323–2342, <https://doi.org/10.1055/s-0035-1561649>.
- [16] C. Walling, A.A. Zavitsas, The copper-catalyzed reaction of peresters with hydrocarbons, *J. Am. Chem. Soc.* 85 (1963) 2084–2090, <https://doi.org/10.1021/ja00897a013>.
- [17] J.K. Kochi, H.E. Mains, Studies on the mechanism of the reaction of peroxides and alkenes with copper salts, *J. Org. Chem.* 30 (1965) 1862–1872, <https://doi.org/10.1021/jo01017a036>.
- [18] M.B. Andrus, A.B. Argade, X. Chen, M.G. Pamment, The asymmetric Kharasch reaction. Catalytic enantioselective allylic acyloxylation of olefins with chiral copper(I) complexes and *tert*-butyl perbenzoate, *Tetrahedron Lett.* 36 (1995) 2945–2948, [https://doi.org/10.1016/0040-4039\(95\)00444-H](https://doi.org/10.1016/0040-4039(95)00444-H).
- [19] K. Smith, C.D. Hupp, K.L. Allen, G.A. Slough, Catalytic allylic amination versus allylic oxidation: a mechanistic dichotomy, *Organometallics* 24 (2005) 1747–1755, <https://doi.org/10.1021/om049052d>.
- [20] J.A. Mayoral, S. Rodríguez-Rodríguez, L. Salvatella, Theoretical insights into enantioselective catalysis: the mechanism of the Kharasch–Sosnovsky reaction, *Chem. Eur. J.* 14 (2008) 9274–9285, <https://doi.org/10.1002/chem.200800638>.
- [21] P. Cancino, V. Paredes-García, P. Aguirre, E. Spodine, A reusable CuII based metal–organic framework as a catalyst for the oxidation of olefins, *Catal. Sci. Technol.* 4 (8) (2014) 2599–2607, <https://doi.org/10.1039/C4CY00152D>.
- [22] D. Saha, T. Maity, R. Sen, Heterogeneous catalytic epoxidation of olefin over a hydrothermally synthesized 3D phosphate bridged copper(II) framework, *J. Coord. Chem.* 66 (14) (2013) 2444–2454, <https://doi.org/10.1080/00958972.2013.806654>.
- [23] A.I. Cánepa, C.M. Chanquía, G.A. Eimer, S.G. Casuscelli, Oxidation of olefins employing mesoporous molecular sieves modified with copper, *Appl. Catal. A* 462–463 (2013) 8–14, <https://doi.org/10.1016/j.apcata.2013.04.031>.
- [24] J.M. Gatica, A.L. García-Cabeza, M.P. Yeste, R. Marín-Barrios, J.M. González-Leal, G. Blanco, G.A. Cifredo, F.M. Guerra, H. Vidal, Carbon integral honeycomb monoliths as support of copper catalysts in the Kharasch–Sosnovsky oxidation of cyclohexene, *Chem. Eng. J.* 290 (2016) 174–184, <https://doi.org/10.1016/j.cej.2016.01.037>.
- [25] A.L. García-Cabeza, R. Marín-Barrios, F.J. Moreno-Dorado, M.J. Ortega, H. Vidal, J.M. Gatica, G.M. Massanet, F.M. Guerra, Acyloxylation of 1,4-dioxanes and 1,4-dithianes catalysed by a copper-iron mixed oxide, *J. Org. Chem.* 80 (2015) 6814–6821, <https://doi.org/10.1021/acs.joc.5b01043>.
- [26] A.L. García-Cabeza, R. Marín-Barrios, R. Azarken, F.J. Moreno-Dorado, M. J. Ortega, H. Vidal, J.M. Gatica, G.M. Massanet, F.M. Guerra, DoE (Design of Experiments) assisted allylic hydroxylation of enones catalysed by a copper–aluminum mixed oxide, *Eur. J. Org. Chem.* 36 (2013) 8307–8314, <https://doi.org/10.1002/ejoc.201301145>.
- [27] M.P. Yeste, H. Vidal, A.L. García-Cabeza, J.C. Hernández-Garrido, F.M. Guerra, G. A. Cifredo, J.M. González-Leal, J.M. Gatica, Low temperature prepared copper-iron mixed oxides for the selective CO oxidation in the presence of hydrogen, *Appl. Catal. A* 552 (2018) 58–69, <https://doi.org/10.1016/j.apcata.2017.12.012>.
- [28] C. Agrafiotis, A. Tsetsekou, The effect of powder characteristics on washcoat quality. Part I: alumina washcoats, *J. Eur. Ceram. Soc.* 20 (2000) 815–824, [https://doi.org/10.1016/S0955-2219\(99\)00218-6](https://doi.org/10.1016/S0955-2219(99)00218-6).
- [29] D.M. Gómez, J.M. Gatica, J.C. Hernández-Garrido, G.A. Cifredo, M.A. Montes, O. Sanz, J.M. Rebled, H. Vidal, A novel CoOx/La-modified-CeO<sub>2</sub> formulation for powdered and washcoated onto cordierite honeycomb catalysts with application in VOCs oxidation, *Appl. Catal. B* 144 (2014) 425–434, <https://doi.org/10.1016/j.apcatb.2013.07.045>.
- [30] P. Ávila, M. Montes, E. Miró, Monolithic reactors for environmental applications: a review on preparation technologies, *Chem. Eng. J.* 109 (2005) 11–36, <https://doi.org/10.1016/j.cej.2005.02.025>.